Eur. J. Mineral.
2010, **22**, 293–304
Published online February 2010

Garutiite, (Ni,Fe,Ir), a new hexagonal polymorph of native Ni from Loma Peguera, Dominican Republic

ANDREW M. MCDONALD[1,*], JOAQUIN A. PROENZA[2], FEDERICA ZACCARINI[3], NIKOLAY S. RUDASHEVSKY[4], LOUIS J. CABRI[5], CHRIS J. STANLEY[6], VLADIMIR N. RUDASHEVSKY[4], JOAN C. MELGAREJO[2], JOHN F. LEWIS[7], FRANCISCO LONGO[8] and RONALD J. BAKKER[3]

[1] Department of Earth Sciences, Laurentian University, 935 Ramsey Lake Road, Sudbury, Ontario P3E 2C6, Canada
*Corresponding author, e-mail: amcdonald@laurentian.ca
[2] Departament de Cristallografia, Mineralogia i Dipòsits Minerals, Facultat de Geologia, Universitat de Barcelona, C/Martí i Franquès s/n, E–08028 Barcelona, Spain
[3] Department of Applied Geological Sciences and Geophysics, The University of Leoben, P. Tunner Str. 5, A–8700 Leoben, Austria
[4] Center for New Technologies, Roentgena Street, 1 197101, St. Petersburg, Russia
[5] Cabri Consulting Inc., 99 Fifth Avenue, Suite 122, Ottawa ONo K1S 5P5, Canada
[6] Mineralogy Department, Natural History Museum, Cromwell Road, London SW7 5BD, UK
[7] Department of Earth and Environmental Sciences, The George Washington University, Washington, DC 20052, USA
[8] Falcondo XStrata Nickel, Box 1343, Santo Domingo, Dominican Republic

Abstract: Garutiite (Ni,Fe,Ir) is a new hexagonal polymorph of native Ni discovered in chromitite from Loma Peguera, Dominican Republic. The mineral was identified in heavy mineral concentrates obtained through the use of electric pulse disaggregation (EPD) and hydroseparation (HS) techniques. It forms as anhedral, botryoidal grains typically 10–60 μm in size (maximum of 110 μm). Grains are single or composite, frequently porous and zoned, and occasionally display an unusual lamellar internal texture. Associated minerals include hexaferrum, ferrian chromite, chlorite-group minerals, serpentine-group minerals, awaruite, irarsite, laurite, native Ru and unidentified species including Ru–Os–Ir-Fe and Pt–Ni–Fe–Ir compounds, $Pt(Ni,Fe)_3$, $(Fe,Ru,Ni,Os,Ir,Co)_2S$ and RhNiAs. The mineral is megascopically grey to grey-black with a metallic luster. In plane-polarized light, garutiite is white in color, exhibits a very weak anisotropy, and no pleochroism, bireflectance or internal reflections were observed. No cleavage was noted and the hardness could not be determined owing to the porous nature of the mineral. The calculated density is 11.33 (1) g/cm^3. Reflectance values (%) in air are: 63.8 at 470, 65.9 at 546, 67.0 at 589 and 68.0 at 650 nm. The average result of electron microprobe analyses ($n =$ 42 from 27 grains) is: Ni 27.91, Fe 19.94, Ir 43.78, Pt 6.98, Co 0.55, Cu 0.43, Ru, 0.50, Rh 0.74, Os 0.67, total 101.51 wt%, corresponding to $(Ni_{0.421}Fe_{0.316}Ir_{0.202}Pt_{0.032}Co_{0.008}Cu_{0.006}Rh_{0.006}Ru_{0.004}Os_{0.003})_{\sum 1}$ or the simplified formula, (Ni,Fe,Ir). Garutiite is the Ni analogue of hexaferrum, osmium and ruthenium and is classified as belonging to the osmium group. As such, the mineral is considered to be hexagonal, crystallizing in space group $P6_3/mmc$ with a 2.6941(4) and c 4.2731(6) Å, $V = 26.86(1)$ Å^3, $Z = 2$. The strongest lines of the X-ray powder diffraction pattern [d(in Å)(I)(hkl)] are: 2.330(50)(100), 2.136(30)(002), 2.046(100)(101), 1.576(30)(102), 1.3470(40)(110), 1.2155(40)(103). Based on its morphology, internal texture, and the associated minerals, garutiite is interpreted to be secondary in origin, *i.e*., having formed at low temperatures during post magmatic processes, such as serpentinization and/or lateritization. The name honors Prof. Giorgio Garuti, in recognition of his contributions to the understanding of the mineralogy of platinum-group elements.

Key-words: garutiite, new mineral species, native nickel, platinum group elements, reflectance data, crystal structure, X-ray diffraction data, osmium group, chromitite, electronic pulse disaggregation, hydroseparation, Loma Peguera, Dominican Republic.

1. Introduction

The earliest reference to native Ni as a mineral species is provided by Ramdohr (1967) who described it as a product related to the low-temperature serpentinization of ophiolites from the Bogota peninsula, near Canala, New Caledonia. Native Ni is a relatively rare mineral that has been identified from only a handful of localities worldwide. In most cases, it appears to be genetically related to the alteration of ultramafic rocks (frequently the process of serpentinization; Hudson & Travis, 1981), more rarely as a product related to meteorite impact events (Jones *et al.*,

DOI: 10.1127/0935-1221/2010/0022-2007
0935-1221/10/0022-2007 $ 5.40

2004) or as a possible high-pressure phase (Van Roermund *et al.*, 2001). Where associated with serpentinization, native Ni is frequently intimately intergrown with heazlewoodite or located in close proximity to this mineral, suggesting that it is the product related to the oxidation or desulfidation of the precursor heazlewoodite (or possibly, pentlandite, awaruite). Native Ni is generally considered to have cubic symmetry (space group *Fm*3*m*), a feature consistent with its occasional occurrence in idiomorphic crystals exhibiting ''cubic'' forms [possibly the hexaoctahedron {321} and octahedron {111}]. Other occurrences describe the mineral as occurring in flakes and grains (Challis, 1975; Dekov, 2006), with confirmation of the species relying solely on chemical data. Analyses required to ascertain the crystallographic properties of these minerals (*e.g.*, single-crystal X-ray diffractometry) were not conducted. It cannot be stressed strongly enough that the reliable identification of any mineral can only be accomplished through a combination of mineral-chemical and crystallographic data. In this present study, we report on the discovery of a new hexagonal polymorph of native Ni, garutiite, [(Ni,Fe,Ir)].

The mineral is named for Prof. Giorgio Garuti (born 1945) in recognition of his contributions to the understanding of the mineralogy of platinum-group elements (PGE). Prof. Garuti has been very active in the investigation of ore deposits related to mafic-ultramafic rocks. The mineral and name have been approved by the Commission on New Minerals, Nomenclature and Classification of the International Mineralogical Association (IMA 2008-055). The type specimen is housed in the Mineralogical Museum of Leoben, Austria (catalogue number 8241). The holotype (the crystal chosen for the X-ray powder diffraction work) is housed at the Canadian Museum of Nature (CMNMC 86089).

2. Occurrence and sample preparation

The Loma Peguera chromitites are found in the central part of Loma Caribe peridotite in the Cordillera Central of the Dominican Republic (Proenza *et al.*, 2007; Zaccarini *et al.*, 2009). Most of the ultramafic rocks consist of harzburgite, dominantly clinopyroxene-rich harzburgite with small amounts of dunite and lherzolite, and are considered to represent the mantle sequence of an ophiolite (Lewis & Jimenez, 1991; Lewis *et al.*, 2006). They have been heavily serpentinized with a well-developed nickel-rich laterite having developed over them. The Ni-laterite deposits occur in the saprolite horizon below a relatively thin cover of ''limonite''. They are considered to be of the hydrous silicate-type, with the main Ni-bearing minerals being hydrated Mg-Ni silicates (serpentine and ''garnierites''; Lewis *et al.*, 2006; Proenza *et al.*, 2008).

In the mid-90's, during exploration and mining activity in the area of Loma Peguera, relatively small lensoidal bodies (<2 m) of chromitite were found associated. They are randomly distributed, typically occurring as discontinuous pods or lenses within small masses of serpentinized dunite that are in turn hosted by serpentinized harzburgite.

The chromitite (>95 vol% chromite) displays massive textures with individual chromite grains showing evidence for development of thin rims of ferrian chromite. No traces of primary silicate minerals were preserved in the matrix of the chromitites and intergranular minerals consist primarily of chlorite-with minor serpentine-group minerals (Proenza *et al.*, 2007).

The chromitite is characterized by relatively high Cr_2O_3 (*Cr#* = 0.75–0.78), Fe_2O_3 (av. 7.8 wt%), TiO_2 (av. = 0.84 wt%) and total PGE (up to more than 3 ppm) contents, compared with values typical of ophiolitic chromitites hosted in mantle peridotites (Proenza *et al.*, 2007). All serpentinized ultramafic rocks around the chromitite bodies have been saprolitized, a process characterized by the preservation of the primary fabric, a marked reduction in the quantity of primary minerals present and the exclusive formation of alteration minerals in the most fractured zones.

To better understand the platinum-group mineralogy of the chromitite and to investigate the broader role that lateritic weathering can play in the formation of secondary PGM, heavy mineral separates were produced *via* a combination electric pulse disaggregation (EPD; *e.g.*, Rudashevsky *et al.*, 1995), and hydroseparation (HS) techniques (Rudashevky *et al.*, 2001a and b, 2002; Cabri *et al.*, 2005a; Rudashevsky & Rudashevsky, 2006, 2007). Whereas HS has been used to concentrate minerals for a number of years, (*e.g.*, Rudashevsky *et al.*, 2004; Cabri *et al.*, 2005b; McDonald *et al.*, 2005, 2008), only a few studies have used EPD and HS in combination (*e.g.*, Cabri *et al.*, 2008a and b; Oberthür *et al.*, 2008). This is the first report of a new mineral having been found after the complementary use of EPD and HS techniques.

Fig. 1. Chromitite pod in laterite, Loma Peguera, Dominican Republic.

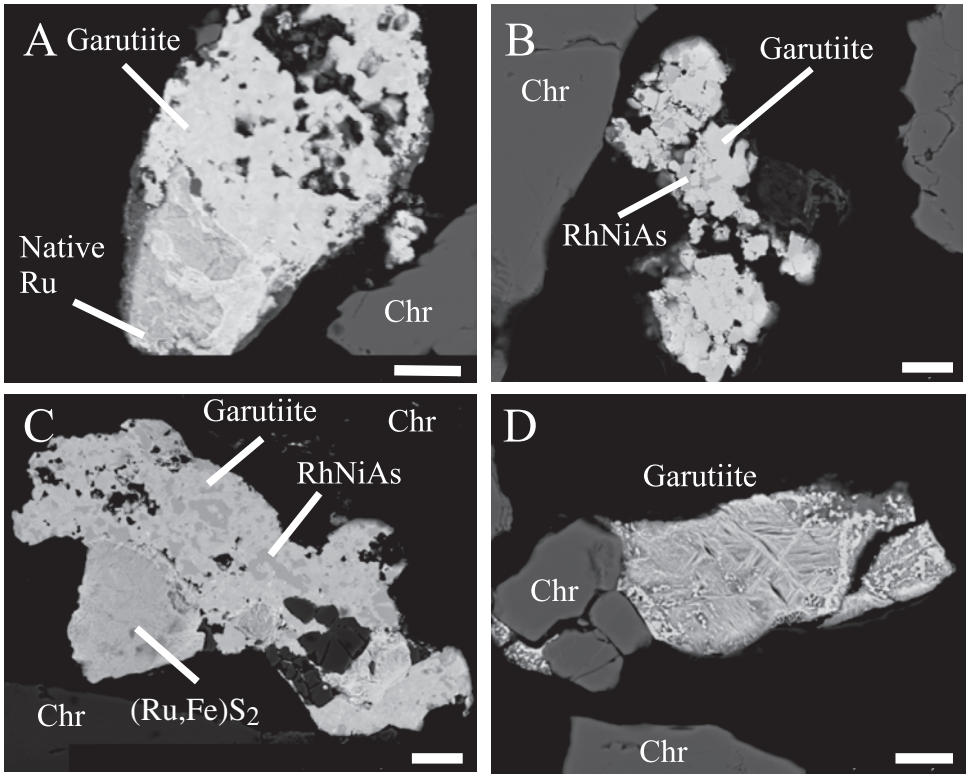

Fig. 2. Back scattered electron images of garutiite associated with native Ru, chromite, unknown RhNiAs and unknown $(Fe,Ni,Ru,Os,Co)_2S$. Scale bar = 10 μm.

A sample (~3.3 kg) of massive chromitite (Fig. 1) was collected from an area located approximately 10 km SE of the town of Bonao (coordinates: latitude 18.9900523°, longitude −70.322982°), Dominican Republic. The sample was processed at the St. Petersburg laboratory of CNT Mineral Consulting Inc. (CNT-MC) first using EPD, a technique that liberates accessory minerals from their host matrix using high voltage without breakage of the crystals and a low production of dust. Subsequently, the heavy-mineral components of the sample were concentrated using a CNT-HS11 hydroseparator, a process that uses a controlled water flow to simulate the action of waves on natural beach placers. The combination of these two techniques resulted in the liberation and concentration of more than 300 individual heavy-mineral grains ranging from 20 to 120 μm in size. The PGM, dominated by Ru-, Os- and Ir-bearing minerals, predominantly occur in the 25–50 μm size fraction. They can be divided into two broad categories: (1) PGM within chromite, including $(Rh,Os,Ir)S_2$ (laurite-erlichmanite?), $(Ir,Ru,Rh,Pt)AsS$ (irarsite?) and an undetermined phase, $(Rh,Ir)_3As_2$ and (2) PGM not encapsulated within the chromite, including several unidentified Pt–Fe–Ni–Ir (isoferroplatinum? tetraferroplatinum?) and Ru–Os–Ir–Rh phases, as well as native Ru (Proenza *et al*., 2007). The non-PGM constituents include a silicate-mineral assemblage, primarily of serpentine- and chlorite-group minerals with minor olivine and quartz and a non-silicate assemblage, including ferrian chromite, magnetite, goethite and awaruite, as well as hexaferrum (hexagonal native Fe), and alloys of Fe–Cr along with native Cu, Sn, Pb and garutiite.

Approximately 20 grains of garutiite were discovered. They typically occur in complex intergrowths with other PGM, along with awaruite, ferrian chromite and chlorite-group minerals and only rarely as single-phase grains. The specific PGM assemblage intimately associated with garutiite includes native Ru and several unidentified phases, including porous and potentially oxygenated compounds of (Ru–Os–Ir–Fe), and two minerals characterized by the stoichiometries $(Fe,Ru,Ni,Os,Ir,Co)_2S$ and RhNiAs (Zaccarini *et al*., 2009). Grains of garutiite are anhedral and botryoidal, frequently porous, zoned and occasionally display an unusual lamellar internal texture (*e.g.*, Fig. 2d). In light of the associated mineralogy, the internal morphology (high porosity, zonation) of individual crystals and its environment of formation, garutiite is interpreted to be secondary in origin, *i.e*. formed at low temperatures during alteration of the ophiolitic host rock.

3. Physical and optical properties

Garutiite forms anhedral, botryoidal grains that are generally 10–60 μm in size, with a maximum of 110 μm. As noted above, the mineral most frequently occurs intergrown with other PGM and intermetallic phases (Fig. 3), a feature making detailed physical analyses on garutiite difficult. Megascopically, the mineral is grey to grey-black in color with a metallic luster. In plane-polarized reflected

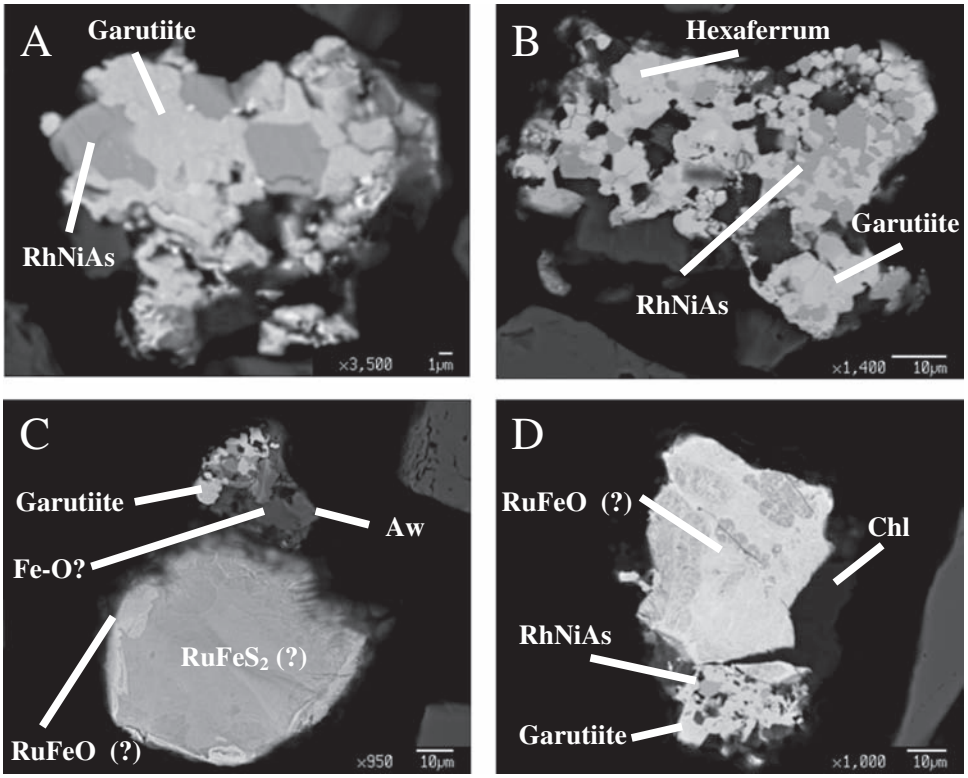

Fig. 3. Back scattered electron images of garutiite associated with native Ru, hexaferrum, awaruite, a chlorite-group mineral, chromite, an unidentified Fe oxide (''Fe–O''), unknown RhNiAs and unknown $(Fe,Ni,Ru,Os,Co)_2S$. Scale bar = 10 μm.

light, it is white with a very weak anisotropy. No bireflectance, pleochroism or internal reflections were observed. It is rather difficult to generalize on the optical properties of garutiite since it is far from being an end-member. To summarize, it has very weak (not measurable on the only grain from which meaningful results could be obtained) bireflectance, which is not dissimilar to that reported for hexaferrum and osmium. Iridian osmium has somewhat greater bireflectance and measurable pleochroism. The properties of hexaferrum are quite variable, depending on its chemistry: Ru-rich hexaferrum is strongly anisotropic, with polarization colors ranging from blue-grey to muddy-brown yellow, while both the Os- and Ir-rich varieties are both weakly anisotropic and show no bireflectance (Mochalov *et al.*, 1998). Whereas osmium and hexaferrum should appear white in color, as reflected in the low dispersion of their spectra, garutiite appears white to slightly cream, but again, the dispersion is weak and the observed color is more likely to be influenced by the other minerals surrounding it. No twinning or cleavage was observed. The density could not be directly measured owing to the complex intergrowth nature of the mineral and its small grain size. The calculated density is 11.33 (1) g/cm^3, based on the empirical formula and unit-cell parameters acquired from X-ray powder diffraction data. No micro-hardness measurements were made. Garutiite was investigated by Raman spectroscopy, using a LABRAM (ISA Jobin Yvon) instrument and a frequency-doubled 100 mW Nd-YAG laser with an excitation of wavelength $\lambda = 532.6$ nm. The obtained Raman spectrum shows no discernible absorption bands over the range of 150–2000 cm^{-1}. Reflectance data over the range 400–700 nm (Table 1; for grain LP 126 gr9) were obtained in air using a Zeiss Axiotron microscope equipped with a Crystal Structures (Lanham) specimen–standard leveling superstage and a J & M Tidas diode array spectrometer. Measurements were made relative to a Zeiss WTiC standard using Cavendish Instruments Onyx software at intervals of 0.823 nm from 400–700 nm, following the procedure described by Stanley *et al.* (2002). The reflectance data and color values of garutiite are listed in Tables 1 and 2, respectively.

4. Chemical composition

Electron-microprobe analyses of garutiite were obtained both on a Superprobe JEOL JXA 8200 (Laboratory Eugen F. Stumpfl, University of Leoben, Austria, operating with an accelerating voltage of 20 kV, a beam current of 10 nA and a beam diameter of 1 μm) and a Cameca SX50 (Serveis Cientificotècnics, University of Barcelona, Spain, operating with an accelerating voltage of 25 kV, a beam current of 20 nA and a beam diameter of 2 μm). In both cases, analyses were made in WDS mode. For analyses made on the JEOL JXA 8200, synthetic NiS (Ni$K\alpha$) and natural chalcopyrite (S$K\alpha$, Fe$K\alpha$, Cu$K\alpha$) were used as standards, along with pure metals for the platinum group elements

Table 1. Reflectance data for garutiite.

λ(nm)	*R*(%)
400	61.9
420	62.3
440	62.9
460	63.5
470	**63.8**
480	64.1
500	64.8
520	65.3
540	65.8
546	**65.9**
560	66.3
580	66.8
589	**67.0**
600	67.2
620	67.6
640	67.8
650	**68.0**
660	68.1
680	68.3
700	68.6

Values given in bold are those recommended by COM, the IMA Commission on Ore Mineralogy.

Table 2. Color values for garutiite.

	A illuminant	C illuminant
x	0.452	0.316
y	0.409	0.322
Y%	66.5	66.2
λ_d	587	578
P_e %	4.3	2.9

(Ir*Lα*, Ru*Lα*, Rh*Lα*, Pt*Lα*, Os*Mα*). The analyzing crystals employed were: PETJ for S, PETH for Ru, Os, Rh, LIF for Cu and LIFH for Ni, Ir and Pt. Automatic on-line corrections were performed for interferences involving Ru-Rh, Ir-Cu and Rh-Pd. On the Cameca SX50 instrument, pure metals were used as standards for Os (Os*Lα*), Ir (Ir*Lα*), Ru (Ru*Lα*), Rh (Rh*Lα*), Pt (Ir*Lα*), Co (Co*Lα*) and Pd (Pd*Lβ*), Cr_2O_3 for Cr (Cr*Lα*), NiO for Ni (Ni*Kα*), FeS_2 for Fe (Fe*Kα*) and S (S*Kα*), $CuFeS_2$ for Cu (Cu*Kα*) and GaAs for As (As*Lβ*). The interferences Ru*Lβ*→Rh*Lα*, Ir*Lα*→Cu*Kα* and Cu*Kβ*→Os*Lα* were corrected on-line. The average (range) from electron microprobe analyses ($n = 42$ from 27 grains) is: Ni 27.91 (22.28–39.20), Fe 19.94 (16.54–22.51), Ir 43.78 (28.98–58.35), Pt 6.98 [*b.d.* (below detection)−24.56], Co 0.55 (*b.d.*−0.82), Cu 0.43 (0.12–0.86), Ru 0.50 (*b.d.*−1.36), Rh 0.74 (0.21–4.66), Os 0.67 (*b.d.*−1.35), total 101.51 wt%, corresponding to the empirical formula, $(Ni_{0.421}Fe_{0.316}Ir_{0.202}Pt_{0.032}Co_{0.008}Cu_{0.006}Rh_{0.006}Ru_{0.004}Os_{0.003})_{\sum = 1}$ and the simplified formula, (Ni,Fe,Ir). The presence of appreciable amounts of Pt (up to 24.56 wt%) and Rh (up to 4.66 wt%) in some analyses are noteworthy. The average (range) from electron-microprobe analyses ($n = 8$ from 3 grains) for associated hexaferrum is: Fe 23.26 (20.35–28.22), Ni 12.42 (3.41–20.81), Ir 58.07 (50.35–67.94), Pt 0.31 (*b.d.*−0.43), Cu 0.58 (0.37–0.85), Ru 1.24 (0.16–36.1), Rh 3.46 (*b.d.*−7.32), Os 0.54 (*b.d.*−0.71), total 99.88 wt%. The average (range) from electron-microprobe analyses ($n = 16$ from 4 grains) for unidentified Pt–Ir–Ni–Fe alloys associated with garutiite is: Pt 52.39 (23.73–63.20), Ir 0.86 (*b.d.*−22.41), Ni 27.44 (15.77–33.44), Fe 17.55 (15.87–20.47), Cu 1.03 (*b.d.*–1.65), Ru 1.24 (*b.d.*–0.47), Rh 0.48 (0.25–4.42), total 99.75 wt%.

5. Crystallographic data and crystal-structure implications

Initially, the chemical formula for garutiite was considered to be Ni_3Ir and that it might represent a new intermetallic structure type. To investigate this further, a grain of garutiite (LP-6-125-gr9) measuring ∼40 × 50 μm was extracted and studied by single-crystal X-ray diffraction methods (Gandolfi X-ray camera with a diameter of 114.6 mm and Co*Kα* radiation). X-ray data were collected using an image plate and the integration method of Matsuzaki & Shinoda (2004). This use of image plates offers several advantages, including production of results that are at least an order of magnitude more precise than those obtained through traditional methods (Nakamuta, 1993; Stachs & Gerber, 2000). The resulting powder pattern of garutiite gave an excellent spread of X-ray diffraction lines to below $d = 1$ Å (Table 3). Although the observed lines were clearly evident, they are rather diffuse, due either to a high-degree of disorder or microstrain effects. A careful analysis of the resulting X-ray powder diffraction pattern indicated it to be similar to that of hexaferrum, the hexagonal polymorph of native Fe. Hexaferrum is a member of the osmium group that also includes native Os and Ru, all of which isostructural, crystallizing in the space group $P6_3/mmc$ (Table 4). The similarity in X-ray powder patterns for these minerals along with that of garutiite, both in terms of X-ray line intensities and observed *d*-spacings (Table 5) indicate the mineral is a new member of the osmium group, a new hexagonal polymorph of native Ni, which must also crystallize in the space group $P6_3/mmc$. On this basis, the X-ray powder pattern for garutiite was indexed, leading to the refined unit-cell dimensions, *a* 2.6941(4) and *c* 4.2731(6) Å, $V = 26.86(1)$ Å^3, $Z = 2$. It should be noted that two additional reflections of moderate intensity at $d = 2.523$ ($I = 30$) and 1.607 Å ($I = 20$) were also observed, neither of which is consistent with the symmetry and unit cell proposed for garutiite. They do correspond well with two of the strongest lines for hematite, but as the strongest line for hematite (∼$d = 2.70$ Å) was not observed, their true nature remains unresolved. Given the observed X-ray powder diffraction pattern and chemical composition of garutiite, the possibility that the mineral might represent other forms of intermetallics, including native Ni (cubic) or ferronickelplatinum (Pt_2FeNi; tetragonal), was also considered. However, comparison of the X-ray powder diffraction patterns for these minerals and garutiite indicates that this is not the case (Table 5).

Table 3. Powder X-ray data for osmium-group minerals, including garutiite.

Garutiite[a]				Hexaferrum (PDF 54-0704)			Osmium (PDF 00-041-0601)			Ruthenium (PDF 00-06-0663)		
*I*meas	*d*meas(Å)	*d*calc(Å)	*hkl*	*I*meas	*d*meas(Å)	*hkl*	*I*meas	*d*meas(Å)	*hkl*	*I*meas	*d*meas(Å)	*hkl*
50	**2.330**	**2.333**	**100**	50	2.28	100	80	2.363	100	40	2.343	100
30	**2.136**	**2.136**	**002**	60	2.10	002	30	2.166	002	35	2.142	002
100	**2.046**	**2.048**	**101**	100	2.006	101	100	2.071	101	100	2.056	101
30	**1.576**	**1.576**	**102**	30	1.549	102	40	1.594	102	25	1.5808	102
40	**1.3470**	**1.3471**	**110**	30	1.316	110	60	1.364	110	25	1.3530	110
40	**1.2155**	**1.2157**	**103**	30	1.195	103	20	1.232	103	25	1.2189	103
10	1.1669	1.1666	200				10	1.180	200	6	1.1715	200
20	1.1391	1.1395	112	20	1.118	112	50	1.153	112	25	1.1434	112
20	1.1256	1.1254	201	20	1.108	201	40	1.039	201	20	1.1299	201
5	1.0680	1.0683	004				5	1.080	004	4	1.0705	004
5	1.0239	1.0239	202				10	1.035	202	5	1.0278	202
5	0.9715	0.9713	104				5	0.9835	104	6	0.9738	104
							40	0.9135	203	16	0.9056	203
							10	0.8929	210	6	0.8857	210
							50	0.8737	211	25	0.8673	211
							20	0.8472	114	18	0.8395	114
							20	0.8252	212	10	0.8185	212
							20	0.8123	105	16	0.8043	105
							5	0.7974	204			
							10	0.7866	300			

[a]Pattern also includes two lines at $d = 2.523$ and 1.607 Å of moderate intensity (*I*est = 30 and 20, respectively) that are attributed to the presence of an unidentified phase.

Table 4. Comparative data for osmium-group minerals, including garutiite.

	Garutiite	Hexaferrum[a]	Osmium[b]	Ruthenium[c]
Chemical Formula:	(Ni,Fe,Ir)	(Fe,Os,Ru,Ir)	(Os,Ir,Ru)	(Ru,Ir,Os)
Crystal System:	Hexagonal	Hexagonal	Hexagonal	Hexagonal
Space Group:	$P6_3/mmc$	$P6_3/mmc$	$P6_3/mmc$	$P6_3/mmc$
Unit cell:				
a	2.6939(5)	2.64(1)	2.726	2.7058
c (Å)	4.2732(6)	4.20(2)	4.326	4.2819
V (Å^3)	26.86(1)	25.35	27.84	27.15
Z	2	2	2	2

[a]Mochalov *et al.* (1998). Note: Data presented are for Ru-rich hexaferrum
[b]Swanson *et al.* (1955).
[c]Urashima *et al.* (1974).

Minerals of the osmium group possess only one crystallographic site in their crystal structures. The implication is that the complex empirical chemical formula established for garutiite most accurately represents solid solution amongst several end-members rather than uncertainty in the chemical formula or crystal structure of the mineral. Each end-member of the group is therefore defined by a single dominant constituent. This fact, along with the empirical formula for garutiite, also indicates the possibility of there being previously unrecognized hexagonal forms of native Ir and possibly, native Pt.

6. Results and their interpretation

The electron-microprobe analyses of garutiite indicate that the crucial elements involved in its composition are Ni, Fe, Ir and Pt. Since the X-ray diffraction pattern indicates a crystal structure with only one atomic position, a classification on the basis of the possible substitution in the Ni–Fe–Ir–Pt system and the 50 % rule can be proposed. Our data presented in the Ni–Fe–Ir ternary (Fig. 4a) show a solid solution between hexaferrum and garutiite, which is to be expected. This substitution is more linear if Pt is added to Ir (Fig. 4b). While no PGE are therefore essential to garutiite, it is not clear what role (if any) such elements might play in stabilizing the existence of the mineral.

Several analyses show that in some grains the Pt content is higher than Ir. These analyses have been plotted in the ternary diagrams of Ni–Fe–(Ir + Pt) (Fig. 4 c, d and e). These suggest that there is limited substitution between Pt and Ir, whereas the substitution is clear between Pt and (Ni + Fe). However, based on the chemical data presented, it is possible that the hexagonal polymorphs of native Ir and Pt may be found in nature.

It is well known that Raman spectroscopy is very sensitive to the presence of covalent bonding. Actually, if the covalent bond is present in the analyzed material, an interaction between the material and the Raman beam produces a very well-defined and visible spectrum. The Raman spectrum obtained on garutiite is flat, suggesting that the possible bonds present in the new PGM are metallic or ionic in character.

Table 5. Comparison of powder X-ray data for garutiite and chemically related phases.

Garutiite				Nickel[a]			Awaruite[b]			Kamacite[c]			Ferronickel-Platinum[d]		
Ni $P6_3/mmc$				PDF 4-850 Ni $Fm3m$			PDF 38-419 (Ni_3Fe) $Pm3m$			PDF 37–474 (Fe, Ni) $Im3m$			PDF 35–702 Pt_2FeNi $P4/mmm$		
*I*meas	*d*meas(Å)	*d*calc(Å)	*hkl*	*I*meas	*d*meas(Å)	*hkl*	*I*meas	*d*meas(Å)	*hkl*	*I*meas	*d*meas(Å)	*hkl*	*I*meas	*d*meas(Å)	*hkl*
													10	3.660	001
													10	2.752	110
50	**2.330**	**2.333**	**100**												
30	**2.136**	**2.136**	**002**										100	2.192	100
100	**2.046**	**2.048**	**101**	100	2.034	111	100	2.044	111	100	2.028	110			
													50	1.935	020
													10	1.830	002
				42	1.762	200	60	1.772	200	32	1.7905	200			
													30	1.699	021
30	**1.576**	**1.576**	**102**										10	1.509	112
										12	1.434	200	10	1.371	220
40	**1.3470**	**1.3471**	**110**										40	1.324	022
													10	1.294	030
40	**1.2155**	**1.2157**	**103**	21	1.246	220	30	1.253	220				10	1.277	221
10	1.1669	1.1666	200										10	1.221	130
20	1.1391	1.1395	112							18	1.1708	298	30	1.157	013
20	1.1256	1.1254	201										20	1.092	222
5	1.0680	1.0683	004	20	1.0624	311	40	1.069	311						
5	1.0239	1.0239	202	7	1.0172	222	10	1.023	222						
										5	1.0139	200			
5	0.9715	0.9713	104												
				4	0.8810	400				5	0.9070	310			
				14	0.8084	331	10	0.814	331	7	0.8279	222			
				15	0.7880	420	10	0.792	420						

[a]Swanson & Tatge (1953).
[b]Williams (1960).
[c]Keller *et al.* (1986).
[d]Rudashevsky *et al.* (1983).

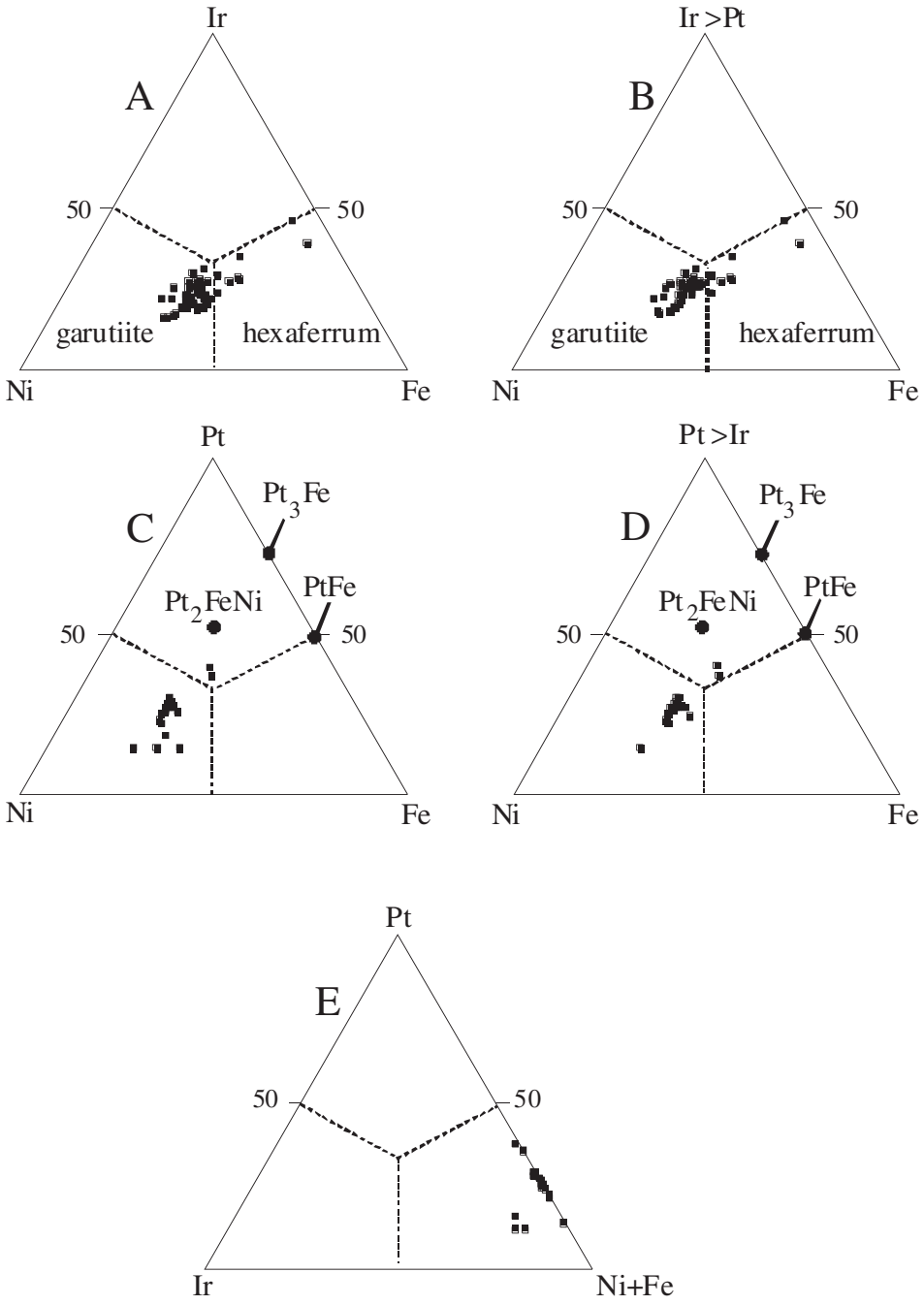

Fig. 4. The compositions of garutiite and hexaferrum (in at. %) plotted in the ternaries: (a) Ni–Fe–Ir, (b) Ni–Fe–(Ir + Pt, Ir > Pt), (c) Ni–Fe–Pt, (d) Ni–Fe–(Pt + Ir, Pt>Ir) and (e) Ir–Pt–(Ni + Fe).

7. Synthesis of hexagonal Ni

The structures of 3*d* metals are generally face-centred cubic (*fcc*) under most conditions (Pearson & Williams, 1979). While the *fcc* structure for synthetic Ni ($a = 3.52$ Å, space group $Fm3m$) is common, the existence of hexagonal-closest packed (*hcp*) Ni has been known for several decades (Hemenger & Weik, 1965), being attributed to epitactic growth, incorporation of impurities, or a low-temperature phase transformation from an amorphous phase (Illy *et al.*, 1999). There are two proposed mechanisms by which it can be synthesized: chemical reduction and epitactic overgrowth. In the former, Ni^{2+} is reduced with a K/B alloy to produce *hcp* Ni powder (Carturan *et al.*, 1988). Mi *et al.* (2005) synthesized *hcp* Ni by reduction of $NiCl_2$ by KBH_4 in ethylenediamine at 300 °C to produce nanoclusters of Ni particles. Importantly, they demonstrated that in the presence of toluene and benzene, only *fcc* Ni was obtained and concluded that impurities in ethylenediamine and organic molecules could be key factors in the stabilization

of nanocrystalline *hcp* Ni. The second mechanism involves epitactic growth of *hcp* Ni on a chemically similar or dissimilar substrate. Meyer *et al*. (1995) were able to produce films of *hcp* Ni on the (001) face of *hcp* Ru. In another study, Tian *et al*. (2005) synthesized *hcp* Ni through deposition and heteroepitactic growth on the (001) face of MgO at 120 πC., producing ''nanosized'' islands of *hcp* Ni crystallites with a thickness of ∼2.5 nm and a lateral size of ∼5 nm. They also found that *fcc* Ni adopted the same surface structure of the substrate, but argued that the oriented *hcp* Ni was energetically more favorable, owing to a smaller lattice mismatch with the substrate relative to *fcc* Ni, and to a small difference in the lattice energies between the *hcp* and *fcc* polymorphs of Ni. While synthetic *hcp* Ni may be produced through reduction of Ni^{2+}, the relatively high temperatures (∼300 °C) and complex K/B compounds required suggest that garutiite is unlikely to have formed through this process. Rather, epitactic nucleation and growth, easily accomplished at relatively low temperatures (∼120 °C), seems more plausible. If the results of Tian *et al*. (2005) are considered, then garutiite may have developed as a highly strained *hcp* polymorph of Ni that, through heteroepitactic growth on a precursor phase, was stabilized. Evidence for such a high-degree of strain could be reflected in broad or diffuse X-ray diffraction lines, as is observed for garutiite. Further, if this is indeed the case, then it may be reasonable to conclude that garutiite developed as unstable nanoparticles that were stabilized by epitactic growth. The nature of the precursor phases is unknown but it is interesting to note that there are many experiments involving the formation of thin films of *hcp* Fe (Prieto *et al*., 1994; Geng *et al*., 2004) and Ni (Meyer *et al*., 1995) on Ru and Rh substrates. It is thus interesting to note that the PGM assemblage associated with garutiite includes several Ru- and Rh- bearing phases, including native Ru, and these may have provided the important substrates required to stabilize garutiite.

8. Mineral paragenesis and genetic implications

The discovery of garutiite was initiated during a broader investigation of platinum group minerals associated with ophiolitic chromitites. In general, these PGM can be grouped into one of two types: (1) primary and (2) secondary (*cf.*, Zaccarini *et al*., 2005). Primary PGM (*e.g.*, laurite, irarsite; Fig. 5) develop during the magmatic stage, prior to and during precipitation of chromite. They occur enclosed by fresh chromite crystals and form small (<10 μm) sub- to euhedral grains. Secondary PGM (*e.g*., native Ru, intermetallic compounds of Ni, Fe and PGE; Fig. 5) form or were modified at relatively low temperature during some post magmatic stage, possibly oceanic serpentinization or weathering (Zaccarini *et al.*, 2009). These are always associated with typical alteration assemblages, including chlorite- and serpentine-group minerals and ferrian chromite. Grains of such PGM tend to be relatively large (∼80–100 μm) and are anhedral. It is in association with secondary PGM that garutiite was discovered. Based on its observed morphology, internal texture and association with alteration minerals, it is postulated that garutiite is also secondary in origin, *i.e*., having formed at low temperatures during post-magmatic processes, such as serpentinization and/or lateritization.

The paragenesis and evolution of PGM and intermetallic phases related to ophiolitic chromitites is both intriguing and complex and has been previously discussed (Garuti & Zaccarini, 1997; Garuti *et al.*, 1999). One of the earliest stages appears to involve the desulfidation or oxidation of existing sulfides, including both primary PGM as well as Fe–Ni sulfides such as pentlandite (Garuti & Zaccarini, 1997). Examples of awaruite overgrowing (replacing?) pentlandite in a veinlet of a serpentine-group mineral have been previously observed at Loma Peguera (Fig. 6). This suggests the possible desulfidation of pentlandite along with a concomitant, preferential release of Fe (*via* oxidation?) to produce awaruite. It has also been previously proposed that awaruite may arise through the desulfidation of heazlewoodite (Ramdohr, 1967). Desulfidation of primary laurite and irarsite may be collectively responsible for the release of Ru, Ir and Os, and to a lesser extent Rh and Pt (González-Jiménez *et al*., 2009). Native Ru has been found to occur in intimate intergrowths with awaruite (Fig. 6) and Ir can be found in relatively high concentrations in later-stage minerals like garutiite. It may be significant that such desulfidized minerals are

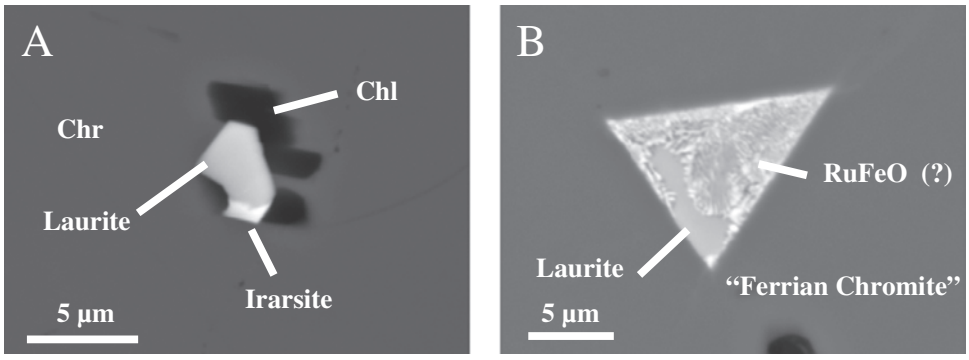

Fig. 5. Back scattered electron image of: (a) primary PGM and (b) secondary PGM in chromite. Loma Peguera, Dominican Republic. Scale bar = 10 μm. Proenza *et al*. (2007).

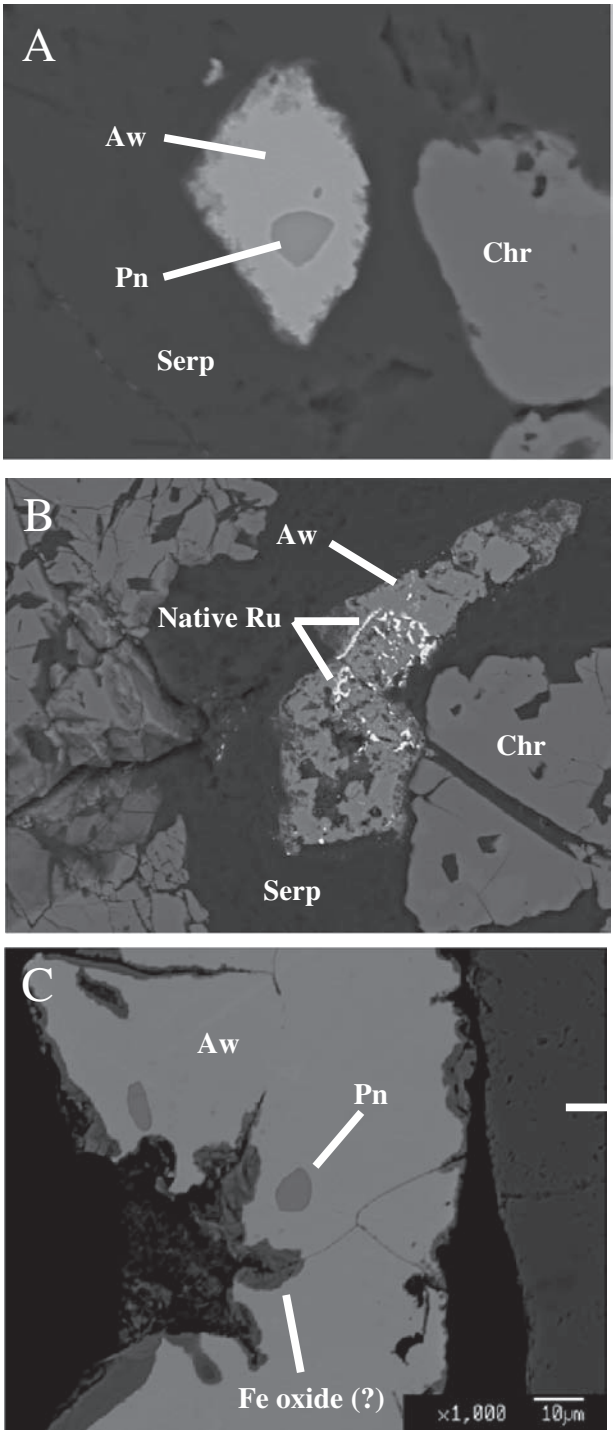

Fig. 6. Back scattered electron images of: (a) awaruite with an inclusion of pentlandite (b) awaruite with inclusions of native Ru surrounded by a serpentine-group mineral (c) inclusion of pentlandite and an unknown Fe-oxide developing along fractures. Loma Peguera, Dominican Republic. Scale bar = 10 µm. Proenza *et al.* (2007).

frequently found surrounded by serpentine-group minerals, suggesting that the process of serpentinization may be directly linked to formation of such minerals. Lastly, in rare instances, garutiite has been observed in association with awaruite and hematite (?). It has been previously proposed that native Ni (cubic) may be produced through the oxidation of awaruite, along with a preferential leaching of Fe (Challis, 1975). Furthermore, some strongly weathered chromitites are found to be associated with chlorite-group minerals, ferrian chromite and abundant ''limonite'' (Garuti & Zaccarini, 1997), implying that oxidation plays an important role in the alteration of chromitites. Considering all these lines of evidence, a plausible paragenetic scenario of (laurite, irarsite) + pentlandite → awarutite + oxygen-bearing (Ru–Ir–Os) alloys → native (Ru,Ir,Os) + garutiite + hematite may be proposed, *i.e.,* a process of desulfidation followed by oxidation. Since the process of serpentinization liberates considerable H_2 during the hydration of olivine (Eckstrand, 1975), resulting in a relative decrease in both Eh and pH, it is highly likely that this process may be a critical step not only in the alteration of primary PGM and sulfides, but also in the production of secondary PGM and intermetallic minerals, the latter including garutiite.

Acknowledgements: The University Centrum for Applied Geosciences (UCAG) is thanked for the access to the Eugen F. Stumpfl electron microprobe Laboratory. We particularly thank Xavier Llovet and Helmut Muehlhans for their assistance during the electron microprobe analyses. This study was funded by the Spanish project CGL2006-07384 and the by the grant SGR00589 of the Catalonian Government. JAP, JFL and FZ are grateful to the staff of Falcondo mine (Xstrata) for their help and hospitality during the sample collection. We also acknowledge the comments of Prof. Werner Paar, an anonymous reviewer and Prof. Ekkehart Tillmanns. Chairman Pete Williams and members of the IMA commission on New Minerals, Nomenclature and Classification are collectively thanked for their unsung efforts in reviewing and providing feedback on the application of garutiite as a new mineral species.

References

Cabri, L.J., Beattie, M., Rudashevsky, N.S., Rudashevsky, V.N. (2005a): Process mineralogy of Au, Pd and Pt ores from the Skaergaard intrusion, Greenland, using new technology. *Miner. Eng.*, **18**, 887–897.

Cabri, L.J., McDonald, A.M., Stanley, C.J., Rudashevsky, N.S., Poirier, G., Durham, B.R., Mungall, J.E., Rudashevsky, V.N. (2005b): Naldrettite, Pd_2Sb, a new palladium antimonide from the Mesamax Northwest deposit, Ungava region, Québec, Canada. *Mineral. Mag.*, **69**, 89–97.

Cabri, L.J., Rudashevsky, N.S., Rudashevsky, V.N., Gorkovetz, V.Ya. (2008a): Study of native gold from the Luopensulo deposit (Kostomuksha area, Karelia, Russia) using a combination of Electric Pulse Disaggregation (EPD) and Hydroseparation (HS). *Miner. Eng.*, **21**, 463–470.

Cabri, L.J., Rudashevsky, N.S., Rudashevsky, V.N., Oberthür, T. (2008b): Electric-Pulse Disaggregation (EPD), Hydroseparation (HS) and their use in combination for mineral processing and advanced characterization of ores. *in* ''Canadian Mineral Processors 40th Annual Meeting, Proceedings'', Paper 14, 211–235.

Carturan, G., Cocco, G., Enzo, S., Ganzerla, R., Lenarda, M. (1988): Hexagonal Close Packed Nickel Powder: synthesis, Structural Characterization and Thermal Behaviour. *Mater. Lett.*, **7**, 47–50.

Challis, G.A. (1975): Native nickel from the Jerry River, South Westland, New Zealand: an example of natural refining. *Mineral. Mag.*, **40**, 247–251.

Dekov, V. (2006): Native nickel in the TAG hydrothermal sediments (Mid-Atlantic Ridge, 26π N): space trotter, guest from the mantle, or widespread mineral connected with serpentinization?. *J. Geophys. Res.*, **111**, B5.

Eckstrand, O.R. (1975): The Dumont serpentinite: a model for control of nickeliferous opaque mineral assemblages by alteration reactions in ultramafic rocks. *Econ. Geol.*, **70**, 183–201.

Garuti, G. & Zaccarini, F. (1997): In situ alteration of platinum-group minerals at low temperature: evidence from serpentinized and weathered chromitite of the Vourinos complex, Greece. *Can. Mineral.*, **35**, 611–626.

Garuti, G., Zaccarini, F., Moloshag, V., Alimov, V. (1999): Platinum-group minerals as indicators of sulfur fugacity in ophiolitic upper mantle: an example from chromitites of the Ray-Iz ultramafic complex, polar Urals, Russia. *Can. Mineral.*, **37**, 1099–1115.

Geng, K.W., He, T., Yang, G.H., Pan, F. (2004): Hexagonal iron formation in Fe/Ru multilayers and its magnetic properties. *J. Magn. Magn. Mater.*, **284**, 26–34.

González-Jiménez, J.M., Proenza, J.A., Gervilla, F., Blanco-Moreno, J.A., Ruíz-Sánchez, R. (2009): Small-scale mobility of platinum-group elements during serpentinization: evidence from the distribution of platinum-group minerals in chromitites from the Sagua de Tánamo district (Mayarí-Baracoa Ophiolite Belt, eastern Cuba). *in* Borg, G., Williams, P. (eds.), ''Smart Sciences for Exploration and Mixing, Proceedings of the 10th Biennial SGA Meeting, Townsville, Australia, 2009'', pp. 319–312.

Hemenger, P. & Weik, H. (1965): On the existence of hexagonal nickel. *Acta Crystallogr.* **19**, 690.

Hudson, D.R. & Travis, G.A. (1981): A native nickel-heazlewoodite-ferroan trevorite assemblage from Mount Clifford, Western Australia. *Econ. Geol.*, **76**, 1686–1697.

Illy, S., Tillement, O., Machizaud, F., Dubois, J.M., Massicot, F., Fort, Y., Ghanbaja, J. (1999): First direct evidence of size-dependent structural transition in nanosized nickel particles. *Philos. Mag.*, **79**, 1021.

Jones, A.P. Kearsley, A., Friend, C.R.L., Robin, E., Beard, A., Tamura, A., Claeys, P. (2004): Paleocene impact ejecta in W. Greenland. *Geophys. Res. Abs.*, **6**, 05063.

Keller, L., Rask, J., Buseck, P. (1986): X-ray powder diffraction data for kamacite. *ICDD Grant-in-Aid Program.*

Lewis, J.F. & Jimenez, J.G. (1991): Duarte Complex in the La Vega – Jarabacoa – Janico area, central Hispaniola; geological and geochemical features of the sea floor during early stages of arc evolution. *in* ''Geologic and Tectonic Development of North America – Caribbean Plate Boundary in Hispaniola'', P. Mann, G. Draper, J.F. Lewis eds., *Geol. Soc. Am. Spec. Pap.*, **262**, 115–141.

Lewis, J.F., Draper, G., Proenza, J.A., Espaillat, J., Jimenez. J. (2006): Ophiolite-related ultramafic rocks (serpentinites) in the Caribbean region: a review of their occurrence, composition, origin, emplacement and nickel laterite soils. *Geol. Acta.*, **4**, 237–263.

Matsuzaki, T. & Shinoda, K. (2004): A method for digitizing the X-ray diffraction pattern on X-ray film by Gandolfi camera. *J. Geosci.*, Osaka City Univ., **47**(1), 1–8.

McDonald, A.M., Cabri, L.J., Stanley, C.J., Rudashevsky, N.S., Poirier, G., Ross, K.C., Mungall, J.E., Durham, B.R., Rudashevsky, V.N. (2005): Ungavaite, Pd_4Sb_3, a new intermetallic mineral from the Mesamax Northwest deposit, Ungava region, Québec, Canada: description and genetic implications. *Can. Mineral.*, **43**, 1735–1744.

McDonald, A.M., Cabri, L.J., Rudashevsky, N.S., Stanley, C.J., Rudashevsky, V.N., Ross, K.C. (2008): Nielsenite, $PdCu_3$, a new platinum-group intermetallic mineral from the Skaergaard Intrusion, Greenland. *Can. Mineral.*, **46**, 709–716.

Meyer, J.A., Schmid, P., Behm, R.J. (1995): Effect of layer-dependent adatom mobilities in heteroepitaxial metal film growth: Ni/Ru(0001). *Phys. Rev. Lett.*, **74**, 3864–3867.

Mi, Y.-Z., Yuan, D.-S., Liu, Y.-L., Zhang, J.-X., Xiao, Y. (2005): Synthesis of hexagonal close-packed nanocrystalline nickel by a thermal reduction process. *Mater. Chem. Phys.*, **89**, 359–361.

Mochalov, A.G., Dmitrenko, G.G., Rudashevsky, N.S., Zhernovsky, I.V., Boldyreva, M.M. (1998): Hexaferrum (Fe,Ru),(Fe,Os),(Fe,Ir) – a new mineral. *Zap. Vseross. Mineral. Obshch.*, **127**(5), 41–51 (*in Russian*).

Nakamuta, Y. (1993): The determination of lattice parameter of a small crystal with Gandolfi camera. *J. Mineral. Soc. Jpn*, **22**(3), 113–122.

Oberthür, T., Melcher, F., Sitnikova, M., Rudashevsky, N.S., Rudashevsky, V.N., Cabri, L.J., Lodziak, J., Klosa, D., Gast, L. (2008): Combination of Novel Mineralogical Methods in the Study of Noble Metal Ores – Focus on Pristine (Bushveld, Great Dyke) and Placer Platinum Mineralisation. *in* ''Ninth International Congress for Applied Mineralogy ICAM 2008'', *Aust. Inst. Min. Metall.*, Publication Series No. 8/2008, 187–194.

Pearson, D.I.C. & Williams, J.M. (1979): ^{57}Fe Mössbauer study of hexagonal phase iron alloys. *J. Phys. F: Met. Phys.*, **9**, 1797–1813.

Prieto, C., De Andres, A., Matrinez, J.L. (1994): Elastic and structural properties of hexagonal Fe/Ru superlattices. *Physica Status Solidi A Appl. Res.*, **146**(2), 613–620.

Proenza, J.A., Zaccarini, F., Lewis, J.F., Longo, F., Garuti, G. (2007): Chromian spinel composition and the Platinum Group Minerals of the PGE-rich Loma Peguera chromitites, Loma Caribe peridotite, Dominican Republic. *Can. Mineral.*, **45**, 631–648.

Proenza, J.A., Lewis, J.F., Galí, S., Tauler, E., Labrador, M., Melgarejo, J.C., Longo, F., Bloise, G. (2008): Garnierite mineralization from Falcondo Ni-laterite deposit (Dominican Republic). *Macla*, **9**, 197–198.

Ramdohr, P. (1967): On the wide-spread paragenesis of ore minerals originating during serpentinization. *Geologiya Rudnykh Mestorozhdenii*, **2**, 32–43 (*in Russian*).

Rudashevsky, N.S. & Rudashevsky, V.N. (2006): Patent of Russian Federation #2281808, invention ''Hydraulic Classifier'', Moscow, 20 August 2006.

—, — (2007): Patent of Russian Federation #69418, industrial (useful) model, ''Device for separation of solid particles'', Moscow, December 27, 2007.

Rudashevsky N.S., Mochalov, A.G., Men'shikov, Y.P., Shumskaya, N.I. (1983): Ferronickelplatinum, Pt_2FeNi, a new mineral species. *Zap. Vseross. Mineral. Obshch.*, **112**, 487–494 (*in Russian*).

Rudashevsky N.S., Burakov, B.E., Lupal, S.D., Thalhammer, O.A.R., Saini-Eidukat, B. (1995): Liberation of accessory minerals from various rock types by electric-pulse disintegration – method and application. *Trans. Inst. Min. Metall. Sec. C. Mineral Proc.. Extract. Metall*., **104**, C25–C29.

Rudashevsky, N.S., Rudashevsky,V.N., Lupal S.D. (2001a): Patent of Russian Federation #2165300, invention ''Hydraulic Classifier'', Moscow, 20 April 2001.

—, —, — (2001b): The method of separating granular materials and device for carrying out said method. Patent Cooperation Treaty (PCT), (16 March 2001) on the basis of Russian patent #2165300, Moscow, 20 April 2001.

Rudashevsky, N.S., Garuti, G., Andersen, J.C.Ø., Kretser, Y.L., Rudashevsky, V.N., Zaccarini, F., (2002): Separation of accessory minerals from rocks and ores by hydroseparation (HS) technology: method and application to CHR-2 chromitite, Niquelandia, Brazil. *Trans. Inst. Min. Metall. Sec. B: Appl. Earth Sci*., **111**, 87–94.

Rudashevsky, N.S., McDonald, A.M., Cabri, L.J., Nielsen, T.D.F., Stanley, C.J., Kretser, Yu.L., Rudashevsky, V.N. (2004): Skaergaardite, PdCu, a new platinum-group intermetallic mineral from the Skaergaard intrusion, Greenland. *Mineral. Mag.*, **68**, 603–620.

Stachs, O. & Gerber, T. (2000): An image plate chamber for X-ray diffraction experiments in Debye-Scherrer geometry. *Rev. Sci. Instrum.*, **71**(11), 4007–4009.

Stanley, C.J., Criddle, A.J., Forster, H.J., Roberts, A.C. (2002): Tischendorfite, $Pd_8Hg_3Se_9$, a new mineral species from Tilkerode, Harz Mountains, Germany. *Can. Mineral*., **40**, 739–745.

Swanson, H.E. & Tatge, E. (1953): Standard X-ray Diffraction Powder Patterns. *Natl. Bur. Stand. (U.S.)* Circ. 539, **I**, 13–47.

Swanson, H.E., Fuyat, R.K., Ugrinic, G.M. (1955): Standard X-ray diffraction powder patterns. *Natl. Bur. Stand. (U.S.)* Circ. 539, **IV**, 8.

Tian, W., Sun, H.P., Pan, X.Q., Yu, J.J., Yeadon, M., Boothroyd, C.B., Feng, Y.P., Lukaszew, R.A., Clarke, R. (2005): Hexagonal close-packed Ni nanostructures grown on the (001) surface of MgO. *Appl. Phys. Lett.*, **86**, 131915.

Urashima, Y., Wakabayashi, T., Masaki, T., Terasaki, *Y.* (1974): Ruthenium, a new mineral from Horokanai, Hokkaldo, Japan. *Mineral. J. (Jpn)*, **7**, 438–444.

Van Roermund, H.L.M., Drury, M.R., Barnhoorn, A., De Ronde, A. (2001): Non-silicate inclusions in garnet from an ultra-deep orogenic periodite. *Geol. J.*, **35**, 209–229.

Williams, K. (1960): An association of awaruite with heazlewoodite. *Am. Mineral.*, **45**, 450–453.

Zaccarini F., Proenza J.A., Ortega-Gutierrez F., Garuti G. (2005): Platinum group minerals in ophiolitic chromitites from Tehuitzingo (Acatlan complex, southern Mexico): implications for post-magmatic modification. *Mineral. Petrol.*, **84**, 147–168.

Zaccarini, F., Proenza, J.A., Rudashevsky, N.S., Cabri, L.J., Garuti, G., Rudashevsky, V.N., Melgarejo, J.C., Lewis, J.F., Longo, F., Bakker, R.J., Stanley, C.J. (2009): The Loma Peguera ophiolitic chromitite (Central Dominican Republic): a source of new platinum group minerals (PGM) species. *N. Jahrb. Mineral. Abh.*, **185/3**, 335–349.

Received 24 July 2009
Modified version received 30 October 2009
Accepted 7 December 2009